Available online at www.sciencedirect.com

ScienceDirect

IFAC PapersOnline CONFERENCE PAPER ARCHIVE

IFAC PapersOnLine 51-29 (2018) 171–176

Navigation filters for Autonomous Underwater Vehicles during geotechnical surveying experiments ⋆

Daniela De Palma and **Giovanni Indiveri**

Dipartimento Ingegneria Innovazione, University of Salento - ISME Node - Lecce, Italy (e-mail: name.lastname@unisalento.it).

Abstract: This paper describes two navigation filters designed for an Autonomous Underwater Vehicle (AUV) for geotechnical surveying. Both a Luenberger observer for a kinematic model of the vehicle as well as an extended Kalman filter for its dynamic model are addressed. The filters allow to fuse information coming from a Global Positioning System (GPS), a compass, a gyro, a depth meter, and acoustic based range measurements. A thruster model mapping low level actuator commands to vehicle surge velocity is also exploited in the design. The performances of both filters have been compared using the experimental data collected during the H2020 WiMUST (Widely scalable Mobile Underwater Sonar Technology) project experiments.

Keywords: Marine systems, autonomous vehicles, navigation.

1. INTRODUCTION

WiMUST (Widely scalable Mobile Underwater Sonar Technology) is a project funded by the European Community within the H2020 framework (Work Programme 2014 - 2015, LEIT- ICT, 5). The main objective of the WiMUST project is the design, the development, and the testing of a robotic system composed of cooperating Autonomous Surface Vehicles (ASVs) and Autonomous Underwater Vehicles (AUVs) to perform geotechnical surveying and geophysical exploration by means of seismic acoustic data acquisition Al-Khatib et al. (2015), Antonelli et al. (2016b), Antonelli et al. (2016a). To the purpose, the WiMUST project (http://www.wimust.eu/) involves four Academic Partners (ISME, IST, CINTAL, UH) and five Industrial Partners (Graaltech, EvoLogics, CGG, Geo Marine, Geosurveys), with specific expertise in the field of marine robotics, acoustic systems, and geophysical and geotechnical surveys.

The WiMUST system is composed of two ASVs carrying a sparker each, and by a fleet of AUVs (i.e., Medusa AUVs Abreu et al. (2016) from IST and Folaga AUVs Caffaz et al. (2010) from ISME and Graaltech) towing streamers equipped with hydrophones to acquire sub-bottom profiling acoustic data. The hydrophones on the streamers towed by the AUVs can be envisioned as an acoustic array that, by means of the autonomous and coordinated motion among ASVs and AUVs, can have different geometries. Indeed, by actively controlling the geometry of the robot formation, it is possible to change the shape of the acoustic array antenna according to the needs of the considered application. Reliable and accurate navigation is of paramount importance in this framework. The WiMUST system architecture allows the involved AUVs to measure range distances from surface beacons (anchor nodes). This is achieved through time of flight measurements of acoustic signals thanks to the use of atomic clocks installed on the AUVs and on the anchor nodes. Details of this measurement system are here omitted for the sake of brevity. Indeed range measurements from a known anchor can be used to support navigation as widely discussed in the marine robotics literature of the last years (refer, by example, to Batista et al. (2011); Webster et al. (2013); Bayat et al. (2016); De Palma et al. (2015); Indiveri et al. (2016); De Palma et al. (2017)).

In this paper we will focus on the navigation filters design for the Folaga AUVs being part of the WiMUST AUVs fleet. Section 2 briefly describes the Folaga platform. Section 3 describes a kinematic model for the vehicle and a kinematic navigation filter, while sections 4 and 5 present a dynamic model for the vehicle and a dynamic navigation filter. Results from sea experiments are reported in section 6. Finally conclusions are summarised in section 7.

2. FOLAGA AUV

The Folaga platform Alvarez et al. (2009) Caffaz et al. (2010) is a cylindrical shaped glider AUV with a rather advanced actuation system. It has a main stern propeller thruster for controlling surge and eight jet pumps for directional control. Four of them are in the stern area and four in the bow. Each of the bow and stern pumps are arranged at ninety degrees one from the other so that two are in the vertical plane and two in the horizontal one. This set up allows to control pitch, yaw, sway and heave. The Folaga is also equipped with a flooding chamber to actively control buoyancy for an additional heave control system. Moreover the internal vehicle battery (one of the heaviest elements of the hardware) is mounted on an actuated moving mechanism allowing to change its

⋆ This work was partially supported by the European Union's Horizon 2020 research and innovation programme under the project WiMUST: Widely scalable Mobile Underwater Sonar Technology, grant agreement N°645141 (call H2020 ICT-23-2014 Robotics).

10.1016/j.ifacol.2018.09.488

position along the length of the vehicle. This affects the position of the center of mass of the AUV resulting in an additional pitch actuation system. Two navigation filters for the Folaga AUV are described in the following. The first is a Luemberger - type estimator based on a kinematics AUV model, while the second integrates a dynamic lumped parameter model with the available navigation sensors resulting in an extended Kalman filter (EKF). Having a lower order and complexity, the kinematic filter is simpler to tune: it was used mostly for GPS aided surface navigation providing a reliable position to compare with the ones generated by the dynamic model based EKF. This latter filter was used during underwater navigation when GPS is not available.

3. SYSTEM MODELING FOR A KINEMATICS OBSERVER DESIGN

The system model exploits two reference frames: a vehicle body fixed one ($<b>$) and an earth fixed one ($<NED>$). The corresponding rotation matrix is denoted as ${}^{b}R_{ned} \in SO(3)$. The following navigation filter design refers to the position variables only of the AUV as attitude is measured on board by an attitude and heading reference system (AHRS). The vehicle kinematics model in frame $<NED>$ results in the following:

$$\dot{\mathbf{x}} = \mathbf{v}_c + \bar{\mathbf{u}} \tag{1}$$

$$\dot{\mathbf{v}}_c = \mathbf{0} \tag{2}$$

being $\mathbf{x} \in \mathbb{R}^3$ the AUV position in $< NED >$, $\bar{\mathbf{u}} \in \mathbb{R}^3$ is the actuated (and commanded) component of the AUV velocity projected in $< NED >$ and $\mathbf{v}_c \in \mathbb{R}^3$ is an unknown velocity component associated to actuation or environmental disturbances as currents. Such term is modelled as unknown and constant in $<NED>$.

The kinematics model used to design the basic navigation filter consists in equations (1 - 2) and an output equation as

$$\mathbf{y} = \mathbf{x}. \tag{3}$$

The horizontal plane components of the position $\mathbf{x}$ are measured by GPS on the surface. The vertical component (i.e. heave) of $\mathbf{x}$ is measured with a pressure gauge. These equations (in frame $<NED>$) can be reformulated in a linear time invariant (LTI) state space setting as follows

$$\mathbf{z} = \begin{pmatrix} \mathbf{x} \\ \mathbf{v}_c \end{pmatrix} \in \mathbb{R}^{6\times 1} \tag{4}$$

$$\dot{\mathbf{z}} = A\,\mathbf{z} + B\,\bar{\mathbf{u}} \tag{5}$$

$$\mathbf{y} = C\,\mathbf{z} \tag{6}$$

being

$$A = \begin{pmatrix} 0_{3\times 3} & I_{3\times 3} \\ 0_{3\times 3} & 0_{3\times 3} \end{pmatrix} \tag{7}$$

$$B = \begin{pmatrix} I_{3\times 3} \\ 0_{3\times 3} \end{pmatrix} \tag{8}$$

$$C = (I_{3\times 3} \;\; 0_{3\times 3})\,. \tag{9}$$

Such model is completely observable. Based on the ($< NED>$ frame) model described in equations (4 - 9), an estimate $\hat{\mathbf{z}}$ of the state vector $\mathbf{z}$ can be derived through a Luenberger observer as follows

$$\dot{\hat{\mathbf{z}}} = A\,\hat{\mathbf{z}} + B\,\bar{\mathbf{u}} + K\,(\mathbf{y} - C\hat{\mathbf{z}}) \tag{10}$$

$$K \in \mathbb{R}^{6\times 3} \;\; : \;\; (A - KC) \text{ is Hurwitz.} \tag{11}$$

The stability condition in equation (11) can always be met given the full observability condition of (A, C). This allows to estimate both the position and the velocity term $\mathbf{v}_c$. In implementing the proposed filter also notice that the commanded (nominal) velocity $\bar{\mathbf{u}}$ is most likely known in body frame and typically corresponds to the commanded surge. Although Folagas can also command sway and heave velocities through the front and rear water-jet actuators, in the reminder of this discussion it is assumed that $\bar{\mathbf{u}}$ refers to the commanded surge only. Being the term $\bar{\mathbf{u}}$ in $<NED>$ frame, this can be computed as

$$\bar{\mathbf{u}} = {}^{ned}R_b\,{}^{b}\bar{\mathbf{u}} \tag{12}$$

where ${}^{b}\bar{\mathbf{u}}$ is the nominal surge speed in body frame, i.e.

$${}^{b}\bar{\mathbf{u}} = (u, 0, 0)^\top. \tag{13}$$

The term u is computed by an experimentally identified model linking thruster commands to steady state AUV surge speed (details about the identification process go beyond the scope of the present paper).

As for the attitude matrix ${}^{ned}R_b$, in the simplest possible navigation filter implementation, this will be directly given by the on board attitude and heading reference system sensor. The described navigation filter allows to estimate the overall vehicle speed in body frame as:

$${}^{b}\dot{\hat{\mathbf{x}}} = {}^{b}\bar{\mathbf{u}} + {}^{b}R_{ned}\,\hat{\mathbf{v}}_c \tag{14}$$

where $\hat{\mathbf{v}}_c$ is extracted from $\hat{\mathbf{z}}$.

4. FOLAGA DYNAMIC MODEL

Following the standard marine vehicle model described in Fossen (2011), the vehicle kinematics and dynamics equations are the following

$$\dot{\boldsymbol{\eta}} = J(\boldsymbol{\eta})\boldsymbol{\nu} \tag{15}$$

$$\boldsymbol{\nu}_r = \boldsymbol{\nu} - \boldsymbol{\nu}_c \tag{16}$$

$$M\dot{\boldsymbol{\nu}}_r + C(\boldsymbol{\nu}_r)\boldsymbol{\nu}_r + D(\boldsymbol{\nu}_r)\boldsymbol{\nu}_r + \mathbf{g}(\boldsymbol{\eta}) = \boldsymbol{\tau} \tag{17}$$

where $\boldsymbol{\eta} = (x, y, z, \phi, \theta, \psi)^\top = (\mathbf{x}^\top, \boldsymbol{\Phi}^\top)^\top$ is the 6D pose in $< NED >$ frame being $\boldsymbol{\Phi} = (\phi, \theta, \psi)^\top$ the attitude modelled with the roll, pitch and yaw angles. Vector $\boldsymbol{\nu} \in \mathbb{R}^6$ is the generalized velocity in body frame, namely $\boldsymbol{\nu} = (\boldsymbol{\nu}_1^\top, \boldsymbol{\nu}_2^\top)^\top$. The term $\boldsymbol{\nu}_1 = (u, v, w)^\top$ is the inertial linear velocity vector projected in body frame (u is surge, v is sway and w is heave). The term $\boldsymbol{\nu}_2 = (p, q, r)^\top$ is the vehicles angular velocity vector in body frame, i.e. $\boldsymbol{\nu}_2 = {}^{b}\boldsymbol{\omega}_{b/ned}$ where

$${}^{b}\dot{R}_{ned}\,{}^{b}R_{ned}^\top = S({}^{b}\boldsymbol{\omega}_{ned/b}) = -S(\boldsymbol{\nu}_2) \tag{18}$$

being $S(\cdot) \in \mathbb{R}^{3\times 3}$ the skew symmetric matrix associated to the cross product $\mathbf{a} \times \mathbf{b} = S(\mathbf{a})\mathbf{b}$ for any $\mathbf{a}, \mathbf{b} \in \mathbb{R}^3$. Moreover, $\boldsymbol{\nu}_c = \begin{bmatrix} {}^{b}R_{ned}\,\mathbf{v}_c \\ 0_{3\times 1} \end{bmatrix}$ is the irrotational ocean current velocity in body frame. Indeed the linear current velocity term $\mathbf{v}_c$ is assumed to be constant in $<NED>$ frame. Vector $\boldsymbol{\nu}_r = (\boldsymbol{\nu}_{r1}^\top, \boldsymbol{\nu}_{r2}^\top)^\top$ is the AUVs *relative* velocity in body frame.

With reference to figure 1, the actuation (allocation) matrix of the Folaga AUV can be written as follows:

Folaga Control Allocation					
Actuation component	Position	Actuator Type	Range value	Resolution	Units
1	Bow Port	Pump	[0,100]	1	adimensional
2	Bow Starboard	Pump	[0,100]	1	adimensional
3	Bow Up	Pump	[0,100]	1	adimensional
4	Bow Down	Pump	[0,100]	1	adimensional
5	Stern Port	Pump	[0,100]	1	adimensional
6	Stern Starboard	Pump	[0,100]	1	adimensional
7	Stern Up	Pump	[0,100]	1	adimensional
8	Stern Down	Pump	[0,100]	1	adimensional
9	Stern	DC Motor Propeller	[0,100]	1	adimensional

Fig. 1. Folaga actuation system in its body frame

$$B = \left[\begin{array}{cccc|cccc|c} 0 & 0 & 0 & 0 & 0 & 0 & 0 & 0 & \beta \\ \alpha & -\alpha & 0 & 0 & \alpha & -\alpha & 0 & 0 & 0 \\ 0 & 0 & \alpha & -\alpha & 0 & 0 & \alpha & -\alpha & 0 \\ \hline 0 & 0 & 0 & 0 & 0 & 0 & 0 & 0 & 0 \\ \hline 0 & 0 & -\alpha b_u & \alpha b_d & 0 & 0 & \alpha s_u & -\alpha s_d & 0 \\ \alpha b_l & -\alpha b_r & 0 & 0 & -\alpha s_l & \alpha s_r & 0 & 0 & 0 \end{array}\right]. \tag{19}$$

where $\alpha > 0$ (in $[N]$) is the proportionality constant between pump commands and generated thrust, $\beta > 0$ (in $[N]$) is the proportionality constant between the propeller command and the generated surge thrust. The parameters b_* and s_* are constants (in $[Nm]$) proportional to the distances of the corresponding pumps to the body frame. Notice that all $\mathbf{u}$ components are nondimensional.

The allocation matrix in equation (19) does not take into account the effects of the flooding chamber status and battery pack position. Indeed, during the experiments under investigation, such actuation components were not used as control inputs, but rather only for calibrating the vehicle to be neutrally buoyant and with zero steady state roll and pitch. Consequently, in the following the vehicle is assumed to have constant weight, buoyancy, and center of mass. Given the definition of B in (19) the generalized force vector $\boldsymbol{\tau}$ in (17) is given by

$$\boldsymbol{\tau} = B\mathbf{u}. \tag{20}$$

Note that $B \in \mathbb{R}^{6\times 9}$ in (19) is singular as roll is not actuated (null fourth row).

5. DYNAMIC NAVIGATION FILTER

With the aim to improve the performance of the basic navigation filter proposed in section 3, we investigated the use of a navigation algorithm based on a dynamic vehicle model (15-17), rather than on a pure kinematic one as reported in (1-2). We are interested in the estimation of the position of the vehicle, the linear relative velocity of the vehicle and the linear velocity of the ocean current. Therefore we will consider only the translational parts of the vectors in equations (15-17). We write the inertia matrix, the Coriolis and centripetal matrix, the hydrodynamic damping matrix, the restoring forces and moments Fossen (2011) and the allocation matrix in (17) in a compact form as:

$$M = \begin{bmatrix} M_{11} & M_{12} \\ M_{21} & M_{22} \end{bmatrix}; C(\boldsymbol{\nu}_r) = \begin{bmatrix} C_{11}(\boldsymbol{\nu}_{r2}) & C_{12}(\boldsymbol{\nu}_{r2}) \\ C_{21}(\boldsymbol{\nu}_r) & C_{22}(\boldsymbol{\nu}_r) \end{bmatrix}; \tag{21}$$

$$D = \begin{bmatrix} D_{11} & D_{12} \\ D_{21} & D_{22} \end{bmatrix}; g(\boldsymbol{\eta}) = \begin{bmatrix} g_1(\boldsymbol{\Phi}) \\ g_2(\boldsymbol{\Phi}) \end{bmatrix}; B = \begin{bmatrix} B_1 \\ B_2 \end{bmatrix}; \tag{22}$$

where each term $M_{ij}, C_{ij}, D_{ij}, B_i$, and g_i is a (3×3) matrix, $\boldsymbol{\eta}$ and $\boldsymbol{\Phi}$ are defined as in (15-17). With regards to the knowledge of the added mass and hydrodynamic parameters in (21), we resort to the values used in the Folaga simulator described in Canepa (2011). Note that for the sake of simplicity, hydrodynamic drag has been modelled with a linear term only. Assuming the attitude and the angular velocity of the vehicle to be measured, the attitude dynamics is completely known. In this hypothesis, the model in equations (15-17) for the linear degrees of freedom results in:

$$\dot{\mathbf{x}} = {}^{ned}R_b\,\boldsymbol{\nu}_{r1} + \mathbf{v}_c \tag{23}$$

$$M_{11}\dot{\boldsymbol{\nu}}_{r1} + M_{12}\dot{\boldsymbol{\nu}}_{r2} + C_{11}(\boldsymbol{\nu}_{r2})\boldsymbol{\nu}_{r1} + C_{12}(\boldsymbol{\nu}_{r2})\boldsymbol{\nu}_{r2} + \\ + D_{11}\boldsymbol{\nu}_{r1} + D_{12}\boldsymbol{\nu}_{r2} + \mathbf{g}_1(\boldsymbol{\eta}) = B_1\mathbf{u} \tag{24}$$

$$\dot{\mathbf{v}}_c = \mathbf{0}. \tag{25}$$

Hence, the model in (23-25) can be rewritten as:

$$\dot{\mathbf{x}} = {}^{ned}R_b\,\boldsymbol{\nu}_{r1} + \mathbf{v}_c \tag{26}$$

$$\dot{\boldsymbol{\nu}}_{r1} = A^*\boldsymbol{\nu}_{r1} + B^*\mathbf{u} + D^* \tag{27}$$

$$\dot{\mathbf{v}}_c = \mathbf{0} \tag{28}$$

where

$$A^* = -M_{11}^{-1}(C_{11}(\boldsymbol{\nu}_{r2}) + D_{11}) \tag{29}$$

$$B^* = -M_{11}^{-1}B_1 \tag{30}$$

$$D^* = -M_{11}^{-1}((C_{12}(\boldsymbol{\nu}_{r2}) + D_{12})\,\boldsymbol{\nu}_{r2} + \mathbf{g}_1(\boldsymbol{\eta})) + \\ - M_{11}^{-1}M_{12}\,\dot{\boldsymbol{\nu}}_{r2}. \tag{31}$$

Note that, even if $\dot{\boldsymbol{\nu}}_{r2}$ in (31) should do not be known, in most cases it can be neglected. Indeed, often the inertia matrix M has a diagonal form, so that the term M_{12} in (31) that multiplies $\dot{\boldsymbol{\nu}}_{r2}$ is a null matrix ($M_{12} = 0_{3\times 3} \Rightarrow M_{12}\,\dot{\boldsymbol{\nu}}_{r2} = \mathbf{0}$). Moreover, the majority of motions of practical interest are straight line trajectories, characterised by a null angular velocity ($\boldsymbol{\nu}_{r2} = \mathbf{0}, \dot{\boldsymbol{\nu}}_{r2} = \mathbf{0}$) or trajectories with constant angular velocity ($\boldsymbol{\nu}_{r2} = \text{constant} \Rightarrow \dot{\boldsymbol{\nu}}_{r2} = \mathbf{0}$), leading both to a null value of $\dot{\boldsymbol{\nu}}_{r2}$.

Defining a state vector as $\mathbf{z} = [\mathbf{x}^\top\ \boldsymbol{\nu}_{r1}^\top\ \mathbf{v}_c^\top]^\top \in \mathbb{R}^9$, the equations (26 - 28) can be reformulated in a linear time variant (LTV) state space setting:

$$\dot{\mathbf{z}} = \begin{bmatrix} \dot{\mathbf{x}} \\ \dot{\boldsymbol{\nu}}_{r1} \\ \dot{\mathbf{v}}_c \end{bmatrix} = \begin{pmatrix} 0_{3\times 3} & {}^{ned}R_b & I_{3\times 3} \\ 0_{3\times 3} & A^* & 0_{3\times 3} \\ 0_{3\times 3} & 0_{3\times 3} & 0_{3\times 3} \end{pmatrix} \begin{bmatrix} \mathbf{x} \\ \boldsymbol{\nu}_{r1} \\ \mathbf{v}_c \end{bmatrix} + \\ + \begin{bmatrix} 0_{3\times 9} \\ B^* \\ 0_{3\times 9} \end{bmatrix} \mathbf{u} + \begin{bmatrix} 0_{3\times 1} \\ D^* \\ 0_{3\times 1} \end{bmatrix}. \tag{32}$$

The measurements available for the navigation filter are:

- position in $<NED>$ frame acquired through GPS while the vehicle is on the surface,
- surge velocity in body frame estimated by a thruster based model linking thruster commands to steady state surge values,
- range measurements from one or more anchor vehicles (ASVs) having known positions, acquired mainly when the vehicle is underwater and has access only to anchors by means of acoustic modems.

Thus, the output equation is given by:

$$\mathbf{y} = \begin{bmatrix} \mathbf{x} \\ u \\ \|\mathbf{x} - \mathbf{x}_{a_1}\| \\ \vdots \\ \|\mathbf{x} - \mathbf{x}_{a_n}\| \end{bmatrix} \tag{33}$$

with $\mathbf{x}_{a_i}$ the positions of the i th anchor vehicle ($i = 1, \ldots, n$) assumed known (they could come, for example, from the GPS onboard the ASV). Given the non linearity of the output equation (33), due to range measurements, an Extended Kalman Filter (EKF) or Unscented Kalman Filter (UKF) (Allotta et al. (2016)) could be used for the estimation of the state variables. Given the time varying and nonlinear nature of the model, its observability properties are non trivial. The observability analysis is here omitted for the sake of brevity. Specific results relative to the observability of range based navigation filters has been already studied by the authors in De Palma et al. (2017); Indiveri et al. (2016); De Palma et al. (2015). Of course, in the absence of range measurements, the output equation becomes linear and a simpler observer like a standard Kalman filter can be adopted as state estimator.

6. EXPERIMENTS

The effectiveness of the proposed dynamic navigation filter has been validated on the experimental data collected during the last WiMUST project trials. Such data include:

- AUV measures of roll, pitch and yaw angles acquired through inertial on board sensors (compass / inclinometer),
- GPS readings when the AUV is on the surface,
- AUV range measurements from two anchors ASV ($n = 2$) acquired through acoustic modems when the vehicle is underwater,
- ASVs (anchors) position acquired through on board GPS,
- AUV surge velocity from a model based on thrusters commands,
- and the command imparted to the AUV thrusters, 8 pumps and 1 propeller, as depicted in figure 1.

These experimental data refer to two hours of lawn mowing motion both on surface and underwater.

During the surface navigation, the Luemberger - type estimator based on the kinematics AUV model was used as navigation filter. The results of such estimator are compared with the ones generated by the dynamic model based filter. Indeed, the experimental data have been post-processed with an EKF applied on the dynamic AUV model (32-33). It should be noted that, in order to implement the dynamic navigation filter described in section 5, the rotation matrix ${}^{ned}R_b$ is computed by exploiting the measures of roll, pitch and yaw angles, while the angular velocity $\boldsymbol{\nu}_{r2}$ has been derived using the relation in (18), and the $\dot{\boldsymbol{\nu}}_{r2}$ has been assumed to be null. Figure 2 reports the trajectory estimated with both filters and the GPS readings when the vehicle is on the surface. Note that no ground truth is available thus the navigation filters are assessed with reference to the GPS data. Figure 3 reports the norm of position errors between the two filter estimates $||\hat{\mathbf{x}}_{kin} - \hat{\mathbf{x}}_{dyn}||$, being $\hat{\mathbf{x}}_{kin}$ and $\hat{\mathbf{x}}_{dyn}$ the estimates obtained with the kinematic and dynamic filter, respectively. The norm of position errors between each filter and the GPS readings are also reported in figure 3, namely $||\hat{\mathbf{x}}_{kin} - \mathbf{x}_{GPS}||$, $||\hat{\mathbf{x}}_{dyn} - \mathbf{x}_{GPS}||$, being $\mathbf{x}_{GPS}$ the GPS reading. The results of both navigation filters are comparable and close to the GPS readings.

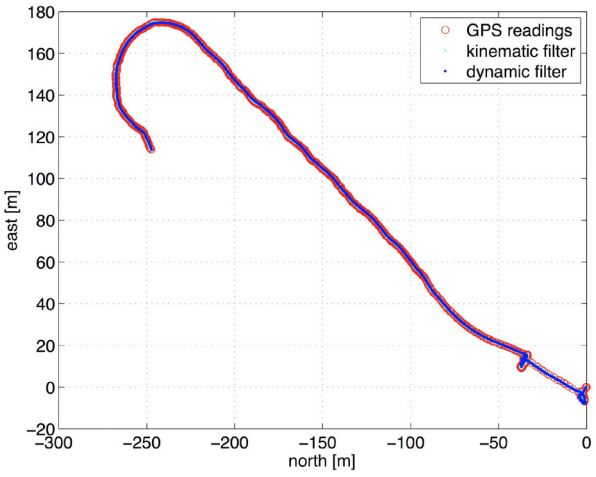

Fig. 2. Filters estimations during surface navigation and GPS readings. The origin in the plot represent the starting point of the vehicle.

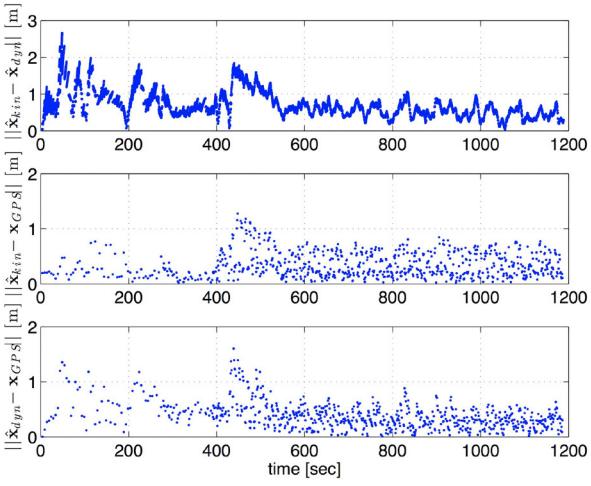

Fig. 3. Norm of error $||\hat{\mathbf{x}}_{kin} - \hat{\mathbf{x}}_{dyn}||$ between kinematic filter estimation and dynamic filter estimation during surface navigation, and norm of position errors between each filter and the GPS reading.

During underwater navigation, range measurements to anchors play an important role since the AUV has no longer access to the GPS readings. In this case the dynamic model based EKF was used. It should be noted that when processing such data, range outliers should be rejected in order not to jeopardise the estimation. Indeed, acoustic measurements are often contaminated by outliers. Here, a few outlier candidate data values have been removed prior to processing the data. Alternative outlier robust filtering techniques are available in the literature (Ruckdeschel et al. (2014); De Palma and Indiveri (2017)) and could

be possibly exploited. The position estimated with the dynamic navigation filter along the whole experiment is shown in figures 4 and 5. In particular, figure 5 highlights the estimations obtained including in the measurement channel the GPS readings when the vehicle is on the surface, and those exploiting the range measurements when the vehicle is underwater. The relative and current velocity estimates are reported in figures 6 and 7, respectively. Interestingly, the resulting estimation appears to be reasonable also during underwater navigation, confirming the effectiveness of the proposed dynamic navigation filter.

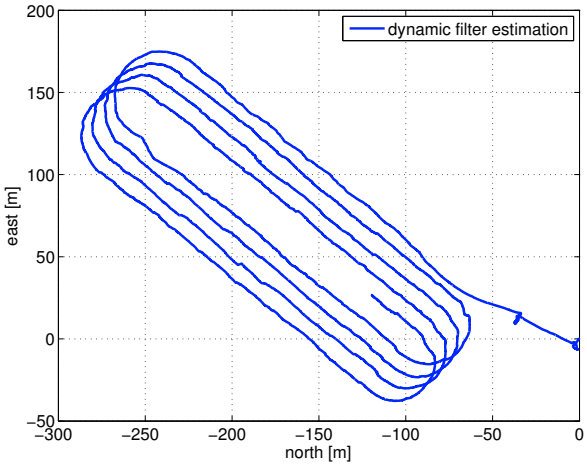

a)

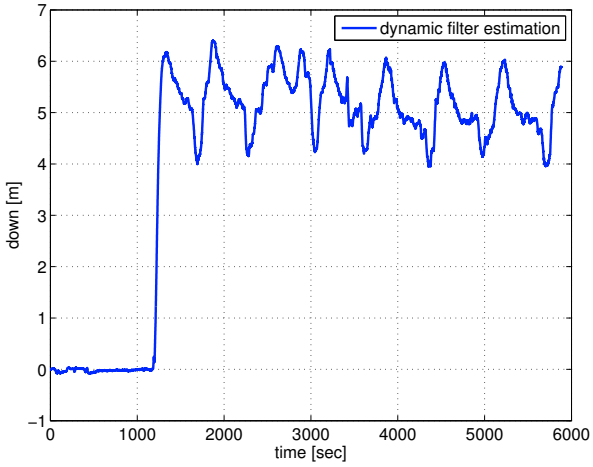

b)

Fig. 4. Vehicle position in $<NED>$ frame estimated using the dynamic navigation filter (EKF estimation): a) north-east components, b) down components.

7. CONCLUSIONS

Two navigation filters designed for the Folaga AUVs within the WiMUST project have been presented in this paper: the first is a Luenberger observer based on a kinematic model of the vehicle; the second is an extended Kalman filter based on a dynamic model of the vehicle. The filters may include measurements from a GPS unit, a compass, a gyro, a depth meter, acoustic based range measurements, and surge velocity estimate from a thruster

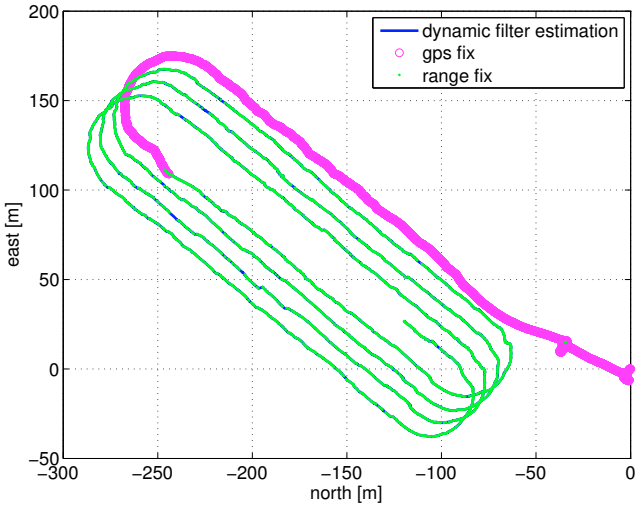

Fig. 5. EKF vehicle position estimates. The magenta circles refer to the filter estimate when measurements include GPS. The green points refer to the filter estimate when underwater and range measurements only are available.

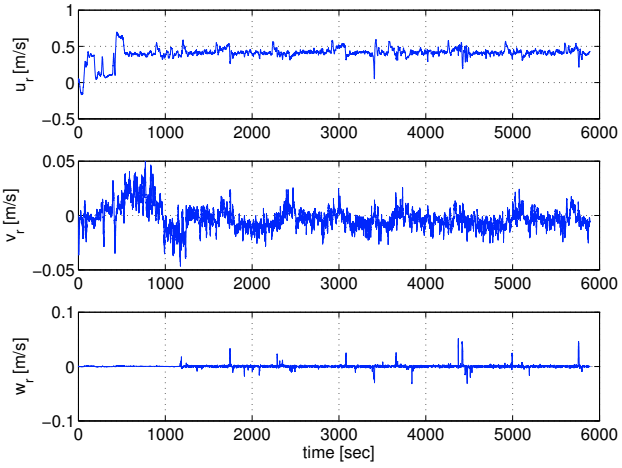

Fig. 6. Vehicle relative velocity $\boldsymbol{\nu}_{r1}$ estimated using the dynamic navigation filter.

based model. The performances of these filters are compared during GPS aided surface navigation based on the experimental data collected during WiMUST trials. Reliable estimations are obtained with both filters. The EKF filter was tested within an underwater navigation scenario, when GPS is not available, exploiting range measurements from surface vehicles. The resulting underwater range-based EKF estimation results reliable and adequate for an AUV based seismic data acquisition task.

REFERENCES

Abreu, P.C., Botelho, J.A., Gois, P., Pascoal, A., Ribeiro, J., Ribeiro, M., Rufino, M., Sebastiao, L., and Silva, H. (2016). The medusa class of autonomous marine vehicles and their role in eu projects. In *Proceedings of MTS/IEEE Oceans '16*. doi:10.1109/OCEANSAP.

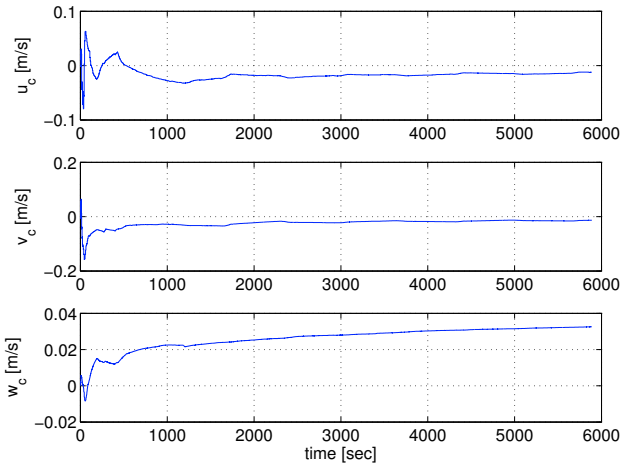

Fig. 7. Current velocity $\mathbf{v}_c$ estimated using the dynamic navigation filter.

2016.7485620. URL http://dx.doi.org/10.1109/OCEANSAP.2016.7485620.

Al-Khatib, H., Antonelli, G., Caffaz, A., Caiti, A., Casalino, G., de Jong, I.B., Duarte, H., Indiveri, G., Jesus, S., Kebkal, K., Pascoal, A., and Polani, D. (2015). The widely scalable mobile underwater sonar technology (WiMUST) project: an overview. In *Proceedings of MTS/IEEE Oceans '15*, 1–5. Genova, Italy. doi:10.1109/OCEANS-Genova.2015.7271688. URL http://dx.doi.org/10.1109/OCEANS-Genova.2015.7271688.

Allotta, B., Caiti, A., Costanzi, R., Fanelli, F., Fenucci, D., Meli, E., and Ridolfi, A. (2016). A new auv navigation system exploiting unscented kalman filter. *Ocean Engineering*, (113), 121–132. doi:10.1016/j.oceaneng.2015.12.058. URL https://doi.org/10.1016/j.oceaneng.2015.12.058.

Alvarez, A., Caffaz, A., Caiti, A., Casalino, G., Gualdesi, L., Turetta, A., and Viviani, R. (2009). Folaga: A low-cost autonomous underwater vehicle combining glider and AUV capabilities. *Ocean Engineering*, 36, 24–38. doi:10.1016/j.oceaneng.2008.08.014. URL http://dx.doi.org/10.1016/j.oceaneng.2008.08.014.

Antonelli, G., Caffaz, A., Casalino, G., Volpi, N.C., de Jong, I.B., De Palma, D., Duarte, H., Grimsdale, J., Indiveri, G., Jesus, S., Kebkal, K., Pascoal, A., Polani, D., and Pollini, L. (2016a). The widely scalable mobile underwater sonar technology (wimust) h2020 project: First year status. In *OCEANS 2016 - Shanghai*, 1–8. doi:10.1109/OCEANSAP.2016.7485587. URL http://dx.doi.org/10.1109/OCEANSAP.2016.7485587.

Antonelli, G., Arrichiello, F., Caffaz, A., Caiti, A., Casalino, G., Volpi, N.C., de Jong, I.B., De Palma, D., Duarte, H., Gomes, J.P., Grimsdale, J., Indiveri, G., Jesus, S., Kebkal, K., Kelholt, E., Pascoal, A., Polani, D., Pollini, L., Simetti, E., and Turetta, A. (2016b). Widely scalable mobile underwater sonar technology: an overview of the H2020 WiMUST project. *Marine Technology Society Journal (Research Initiatives in Europe: Cooperation for Blue Growth)*, 50(4), 42–53. doi:10.4031/MTSJ.50.4.3. URL https://doi.org/10.4031/MTSJ.50.4.3. Guest Editors: Andrea Caiti, Giuseppe Casalino and Andrea Trucco.

Batista, P., Silvestre, C., and Oliveira, P. (2011). Single range aided navigation and source localization: Observability and filter design. *Systems & Control Letters*, 60, 665–673. doi:10.1016/j.sysconle.2011.05.004. URL http://dx.doi.org/10.1016/j.sysconle.2011.05.004.

Bayat, M., Crasta, N., Aguiar, A., and Pascoal, A. (2016). Range-based underwater vehicle localization in the presence of unknown ocean currents: Theory and experiments. *Control Systems Technology, IEEE Transactions on*, 24(1), 122–139. doi:10.1109/TCST.2015.2420636. URL http://dx.doi.org/10.1109/TCST.2015.2420636.

Caffaz, A., Caiti, A., Casalino, G., and Turetta, A. (2010). The hybrid glider/AUV folaga. *Robotics & Automation Magazine, IEEE*, 17(1), 31–44. doi:10.1109/MRA.2010.935791. URL http://dx.doi.org/10.1109/MRA.2010.935791.

Canepa, A. (2011). *GUIDA E CONTROLLO DI VEICOLI SOTTOMARINI AUTONOMI*. Master's thesis, Univesity of Genova, Informatic Engineering.

De Palma, D., Arrichiello, F., Parlangeli, G., and Indiveri, G. (2017). Underwater localization using single beacon measurements: Observability analysis for a double integrator system. *Ocean Engineering*, 142, 650–665. doi:10.1016/j.oceaneng.2017.07.025. URL https://doi.org/10.1016/j.oceaneng.2017.07.025.

De Palma, D. and Indiveri, G. (2017). Output outlier robust state estimation. *International Journal of Adaptive Control and Signal Processing*, 31(4), 581–607. doi:10.1002/acs.2673. URL http://dx.doi.org/10.1002/acs.2673.

De Palma, D., Indiveri, G., and Pascoal, A.M. (2015). A null-space-based behavioral approach to single range underwater positioning. In *10th IFAC Conference on Manoeuvring and Control of Marine Craft MCMC 2015*, volume 48, 55–60. Copenhagen. doi:10.1016/j.ifacol.2015.10.258. URL http://dx.doi.org/10.1016/j.ifacol.2015.10.258.

Fossen, T.I. (2011). *Handbook of Marine Craft Hydrodynamics and Motion Control*. John Wiley & Sons, Ltd. doi:10.1002/9781119994138. URL http://dx.doi.org/10.1002/9781119994138.

Indiveri, G., De Palma, D., and Parlangeli, G. (2016). Single range localization in 3-D: Observability and robustness issues. *Control Systems Technology, IEEE Transactions on*, 24(5), 1853–1860. doi:10.1109/TCST.2015.2512879. URL http://dx.doi.org/10.1109/TCST.2015.2512879.

Ruckdeschel, P., Spangl, B., and Pupashenko, D. (2014). Robust Kalman tracking and smoothing with propagating and non-propagating outliers. *Statistical Papers*, 55(1), 93–123. doi:10.1007/s00362-012-0496-4. URL http://dx.doi.org/10.1007/s00362-012-0496-4.

Webster, S.E., Walls, J.M., Whitcomb, L.L., and Eustice, R.M. (2013). Decentralized extended information filter for single-beacon cooperative acoustic navigation: Theory and experiments. *IEEE Transactions on Robotics*, 29(4), 957–974. doi:10.1109/TRO.2013.2252857. URL http://dx.doi.org/10.1109/TRO.2013.2252857.